NATIONAL ADVISORY COMMITTEE FOR AERONAUTICS

REPORT No. 547

WIND-TUNNEL INTERFERENCE WITH PARTICULAR REFERENCE TO OFF-CENTER POSITIONS OF THE WING AND TO THE DOWNWASH AT THE TAIL

By ABE SILVERSTEIN and JAMES A. WHITE

1935

For sale by the Superintendent of Documents, Washington, D. C. - - - - - - - - - Price 10 cents
Subscription price, $3.00 per year

AERONAUTIC SYMBOLS

1. FUNDAMENTAL AND DERIVED UNITS

	Symbol	Metric		English	
		Unit	Abbreviation	Unit	Abbreviation
Length	l	meter	m	foot (or mile)	ft. (or mi.)
Time	t	second	s	second (or hour)	sec. (or hr.)
Force	F	weight of 1 kilogram	kg	weight of 1 pound	lb.
Power	P	horsepower (metric)		horsepower	hp.
Speed	V	kilometers per hour	k.p.h.	miles per hour	m.p.h.
		meters per second	m.p.s.	feet per second	f.p.s.

2. GENERAL SYMBOLS

W, Weight $= mg$

g, Standard acceleration of gravity $= 9.80665$ m/s^2 or 32.1740 ft./sec.^{2}

m, Mass $= \frac{W}{g}$

I, Moment of inertia $= mk^2$. (Indicate axis of radius of gyration k by proper subscript.)

μ, Coefficient of viscosity

ν, Kinematic viscosity

ρ, Density (mass per unit volume)

Standard density of dry air, 0.12497 kg-m^{-4}-s^2 at 15° C. and 760 mm; or 0.002378 lb.-ft.$^{-4}$ sec.^{2}

Specific weight of "standard" air, 1.2255 kg/m^3 or 0.07651 lb./cu.ft.

3. AERODYNAMIC SYMBOLS

S, Area

S_w, Area of wing

G, Gap

b, Span

c, Chord

$\frac{b^2}{S}$, Aspect ratio

V, True air speed

q, Dynamic pressure $= \frac{1}{2}\rho V^2$

L, Lift, absolute coefficient $C_L = \frac{L}{qS}$

D, Drag, absolute coefficient $C_D = \frac{D}{qS}$

D_o, Profile drag, absolute coefficient $C_{D_o} = \frac{D_o}{qS}$

D_i, Induced drag, absolute coefficient $C_{D_i} = \frac{D_i}{qS}$

D_p, Parasite drag, absolute coefficient $C_{D_p} = \frac{D_p}{qS}$

C, Cross-wind force, absolute coefficient $C_C = \frac{C}{qS}$

R, Resultant force

i_w, Angle of setting of wings (relative to thrust line)

i_t, Angle of stabilizer setting (relative to thrust line)

Q, Resultant moment

Ω, Resultant angular velocity

$\rho\frac{Vl}{\mu}$, Reynolds Number, where l is a linear dimension (e.g., for a model airfoil 3 in. chord, 100 m.p.h. normal pressure at 15° C., the corresponding number is 234,000; or for a model of 10 cm chord, 40 m.p.s. the corresponding number is 274,000)

C_p, Center-of-pressure coefficient (ratio of distance of $c.p.$ from leading edge to chord length)

α, Angle of attack

ϵ, Angle of downwash

α_o, Angle of attack, infinite aspect ratio

α_i, Angle of attack, induced

α_a, Angle of attack, absolute (measured from zero-lift position)

γ, Flight-path angle

REPORT No. 547

WIND-TUNNEL INTERFERENCE WITH PARTICULAR REFERENCE TO OFF-CENTER POSITIONS OF THE WING AND TO THE DOWNWASH AT THE TAIL

By ABE SILVERSTEIN and JAMES A. WHITE
Langley Memorial Aeronautical Laboratory

34653—36——1

NATIONAL ADVISORY COMMITTEE FOR AERONAUTICS

HEADQUARTERS, NAVY BUILDING, WASHINGTON, D. C.

LABORATORIES, LANGLEY FIELD, VA.

Created by act of Congress approved March 3, 1915, for the supervision and direction of the scientific study of the problems of flight. Its membership was increased to 15 by act approved March 2, 1929. The members are appointed by the President, and serve as such without compensation.

TECHNICAL COMMITTEES

AERODYNAMICS
POWER PLANTS FOR AIRCRAFT
AIRCRAFT STRUCTURES AND MATERIALS

AIRCRAFT ACCIDENTS
INVENTIONS AND DESIGNS

Coordination of Research Needs of Military and Civil Aviation

Preparation of Research Programs

Allocation of Problems

Prevention of Duplication

Consideration of Inventions

LANGLEY MEMORIAL AERONAUTICAL LABORATORY

LANGLEY FIELD, VA.

Unified conduct, for all agencies, of scientific research on the fundamental problems of flight.

OFFICE OF AERONAUTICAL INTELLIGENCE

WASHINGTON, D. C.

Collection, classification, compilation, and dissemination of scientific and technical information on aeronautics.

REPORT No. 547

WIND-TUNNEL INTERFERENCE WITH PARTICULAR REFERENCE TO OFF-CENTER POSITIONS OF THE WING AND TO THE DOWNWASH AT THE TAIL

By Abe Silverstein and James A. White

SUMMARY

The theory of wind-tunnel boundary influence on the downwash from a wing has been extended to provide more complete corrections for application to airplane test data. The first section of the report gives the corrections at the lifting line for wing positions above or below the tunnel center line; the second section shows the manner in which the induced boundary influence changes with distance aft of the lifting line.

Values of the boundary corrections are given for off-center positions of the wing in circular, square, 2:1 rectangular, and 2:1 elliptical tunnels. Aft of the wing the corrections are presented for only the square and the 2:1 rectangular tunnels, but it is believed that these may be applied to jets of circular and 2:1 elliptical cross sections. In all cases results are included for both open and closed tunnels.

INTRODUCTION

The influence of wind-tunnel boundaries on the downwash at the lifting line of an airfoil has been the subject of considerable theoretical and experimental study. The investigations have been primarily confined to the problem of determining the average downwash over the span of an airfoil located in the center of a wind-tunnel test section. Prandtl (reference 1) first demonstrated the general method of analysis and gave numerical values for the magnitude of boundary influence on airfoils of finite span tested at the center of either an open or a closed circular tunnel. Glauert, Terazawa, Theodorsen, Rosenhead, and Tani and Sanuki (references 2 to 8) extended this theory to include all the more conventional tunnel sections; that is, square, rectangular, and elliptical. The theoretical results for the central wing position are presented in figure 1 (from reference 9), the circular and square sections being represented by $\lambda=1.0$ for the ellipse and rectangle, respectively.

When testing airplanes and airplane models in wind tunnels, it is often necessary to locate the wing above the horizontal center line of the jet; otherwise at large angles of attack the tail is too near the edge of the air stream. Numerical values of the downwash resulting from the boundary influence have hitherto not been available for off-center positions of the wing. Furthermore, the influence of the boundaries on the downwash behind the wing in the region of the tail has been only briefly and approximately treated (reference 10). This information is necessary for correcting wind-tunnel downwash measurements and elevator angles for flight trim. The theory has therefore been extended to show the magnitude of the boundary influence on airfoils tested above or below the horizontal center line of the tunnel and the dependence of the magnitude of the boundary influence on the distance aft of the wing.

The general problem for any wind tunnel in either the two- or three-dimensional case is that of determining a stream function which, added to that of the flow produced by the airfoil, satisfies the conditions that must exist at the boundaries of the air stream. The effect of the boundaries may then be replaced by this stream function and the boundary-induced velocity computed for any point in the wind tunnel. The conditions at the boundary of the closed tunnel may be exactly expressed as a zero flow normal to the walls; whereas, the open-tunnel boundary condition closely approximates one of constant pressure from the quiescent air around the jet.

In many of the cases of practical importance the solution may be simplified by the use of an external arrangement of vortices that mirror the wing horseshoe vortex in a manner which satisfies the specified boundary conditions. The external image arrangements in these cases are equivalent to the desired stream function.

The value of the interference at any point in a wind tunnel is a function of many factors. Foremost among these factors are: the relative size of the model and the tunnel, the span loading of the airfoil, the test-section shape and constraint, the position of the model in the jet, and the relative location of the point investigated to the airfoil position. Each of these variables has been considered in the present study. The results are presented over a practical range of the ratio of the wing vortex span to the tunnel width for both open and closed tunnels. The span employed is not the geometric one but is an effective span based on the assumption that the wing vortex sheet rolls up into two trailing vortices with a spacing of about 0.8 to 0.9 of the wing length.

The correct ratio of effective to geometric span for various types of loading and aspect ratios is given in reference 2; however, sufficient accuracy for practical purposes is obtained by using a value of 0.8 for a tapered and 0.85 for a rectangular wing. Computations of theoretical boundary influence based on the assumption of a uniform loading over the effective span have shown a close agreement with the calculations based on the actual loading over the geometric span. This assumption is therefore followed throughout the report and it provides a simplification of the problem without a sacrifice of accuracy.

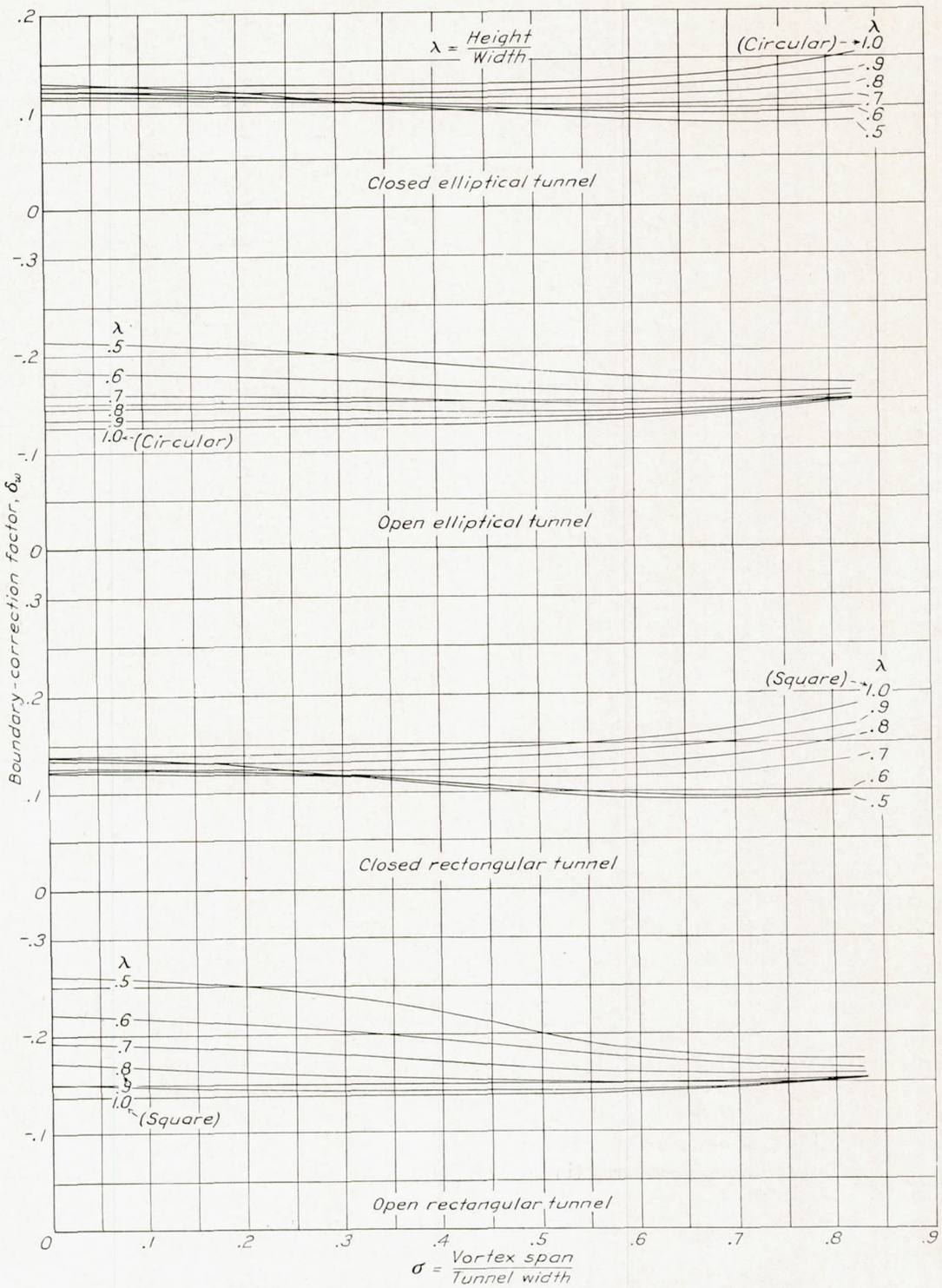

FIGURE 1.—Boundary-correction factors for airfoils of finite span in the center of conventional tunnel sections.

This analysis covers boundary influence on downwash for circular, square, 2:1 elliptical, and 2:1 rectangular tunnels at the wing, and for square and 2:1 rectangular tunnels in the region aft of the wing. The wing positions analyzed are those on the center line and 0.1 and 0.2 of the tunnel height above the center of the jet.

BOUNDARY INFLUENCE AT THE AIRFOIL

Elliptical tunnel.—A general solution for the boundary influence at the lifting line of an airfoil at any position in an elliptical tunnel has been made by Tani and Sanuki (reference 8). The numerical values of the boundary-correction factor δ_w were not given, however, except for the case of the wing on the tunnel center line.

Following the method of Tani and Sanuki, we may write in the elliptical coordinates (ξ, η), for the closed elliptical tunnel,

$$\delta_w=\frac{c}{4a\sigma^2}\left[\sum_{n=1}^{\infty}{}' \frac{e^{-n\xi_0}}{n\cosh n\xi_0}\cosh^2 n\xi_1\cos^2 n\eta_1 + \sum_{n=2}^{\infty}{}'' \frac{e^{-n\xi_0}}{n\sinh n\xi_0}\sinh^2 n\xi_1\sin^2 n\eta_1\right] \tag{1}$$

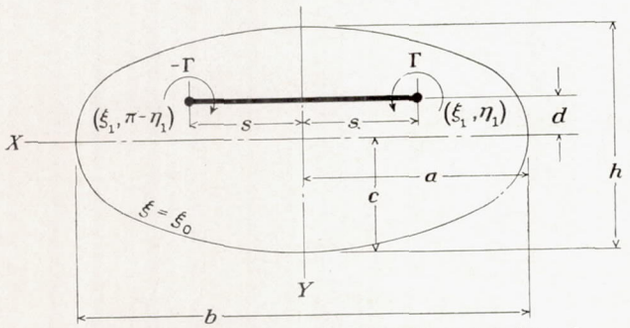

FIGURE 2.—Off-center location of airfoil in an elliptical wind tunnel.

and, for the open elliptical tunnel,

$$\delta_w=-\frac{c}{4a\sigma^2}\left[\sum_{n=1}^{\infty}{}' \frac{e^{-n\xi_0}}{n\sinh n\xi_0}\cosh^2 n\xi_1\cos^2 n\eta_1 + \sum_{n=2}^{\infty}{}'' \frac{e^{-n\xi_0}}{n\cosh n\xi_0}\sinh^2 n\xi_1\sin^2 n\eta_1\right] \tag{2}$$

in which a and c are, respectively, the major and minor semiaxes of the ellipse (fig. 2), and σ is the ratio of the span of the trailing vortices to the tunnel width ($b=2a$). The symbol Σ' implies that only odd values of n are to be summed and Σ'' indicates the use of only even values of n. The usual boundary-correction factor δ_w is defined by

$$\Delta\alpha_w=\delta_w\frac{S}{C}C_L$$

in which S and C are the areas of the wing and test section, respectively, and $\Delta\alpha_w$ is the induced downwash angle at the lifting line of the wing due to the influence of the boundaries. The subscript w refers to the location at the lifting line.

The elliptical coordinates ξ and η are related to the rectangular coordinates x and y as follows:

$$\left.\begin{aligned} x&=k\cosh\xi\cos\eta \\ y&=k\sinh\xi\sin\eta \end{aligned}\right\}$$

in which k is a constant required to preserve the scale of dimensions. The boundary ellipse is defined by $\xi=\xi_0$, so that

$$\begin{aligned} a&=k\cosh\xi_0 \\ c&=k\sinh\xi_0 \end{aligned}$$

or

$$\begin{aligned} \xi_0&=\coth^{-1}\frac{a}{c} \\ k&=\sqrt{a^2-c^2} \end{aligned}$$

The elliptical coordinates (ξ_1, η_1) of the vortex position (x_1, y_1) are given by

$$2\sin^2\eta_1=p\pm\sqrt{p^2+\left(\frac{2y_1}{k}\right)^2}$$

$$\sinh\xi_1=\frac{y_1}{k\sin\eta_1}$$

in which

$$p=1-\left(\frac{x_1}{k}\right)^2-\left(\frac{y_1}{k}\right)^2$$

Substitution of the foregoing values of ξ_0, ξ_1, and η_1 in equations (1) and (2) permits the obtaining of the values of δ_w for the closed and open tunnels. The series converges rapidly and the use of only the first two terms is sufficient.

For an infinitely small airfoil, σ approaches 0 and equations (1) and (2) reduce, for the closed tunnel, to

$$\delta_w=\frac{ac}{4(a^2-c^2)}\left[\sum_{n=1}^{\infty}{}' \frac{ne^{-n\xi_0}\cosh^2 n\xi_1}{\cosh n\xi_0\cosh^2\xi_1}+\sum_{n=2}^{\infty}{}'' \frac{ne^{-n\xi_0}\sinh^2 n\xi_1}{\sinh n\xi_0\cosh^2\xi_1}\right]$$

and for the open tunnel, to

$$\delta_w=-\frac{ac}{4(a^2-c^2)}\left[\sum_{n=1}^{\infty}{}' \frac{ne^{-n\xi_0}\cosh^2 n\xi_1}{\sinh n\xi_0\cosh^2\xi_1} + \sum_{n=2}^{\infty}{}'' \frac{ne^{-n\xi_0}\sinh^2 n\xi_1}{\cosh n\xi_0\cosh^2\xi_1}\right]$$

The values of δ_w are given in figures 3 and 4 plotted against the distance of the airfoil from the center line for the open and closed 2:1 elliptical tunnels. The factors are the same for wing positions above and below the center of the tunnel.

Circular tunnel.—The circular tunnel is a special case of the elliptical tunnel in which the boundary-ellipse parameter ξ_0 approaches ∞, and the values of δ_w for the circular tunnel may thus be computed from equations (1) and (2). A simpler and more direct method of solution is revealed, however, by employing the inverse image method (fig. 5).

Let the effect of the vortex A at a point x of the wing be considered. Since the radius r equals $\sqrt{(x'-x)^2+y'^2}$

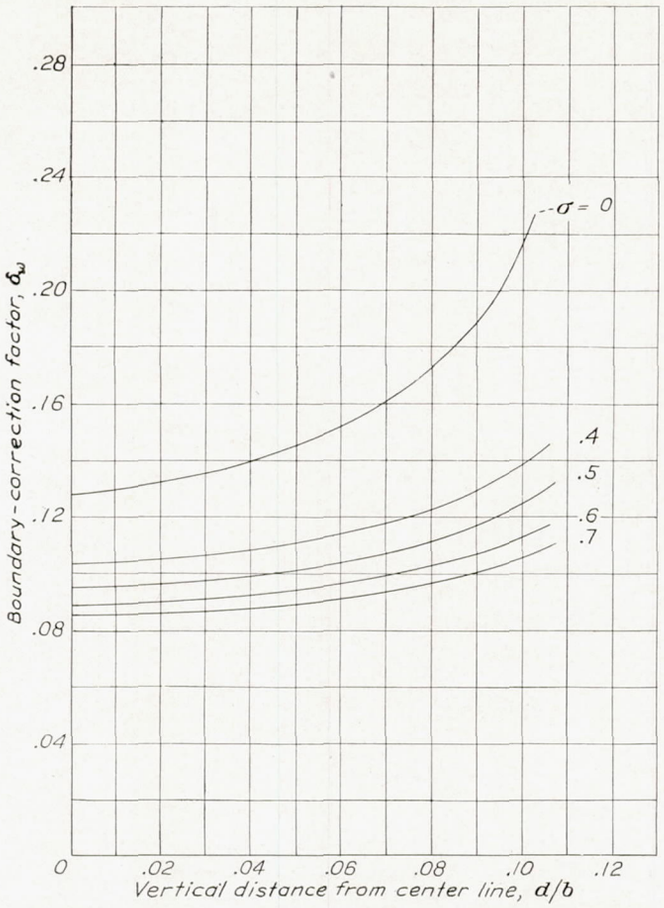

FIGURE 3.—Boundary-correction factors at the airfoil lifting line for the closed 2:1 elliptical tunnel. Airfoil locations are above or below the tunnel center line.

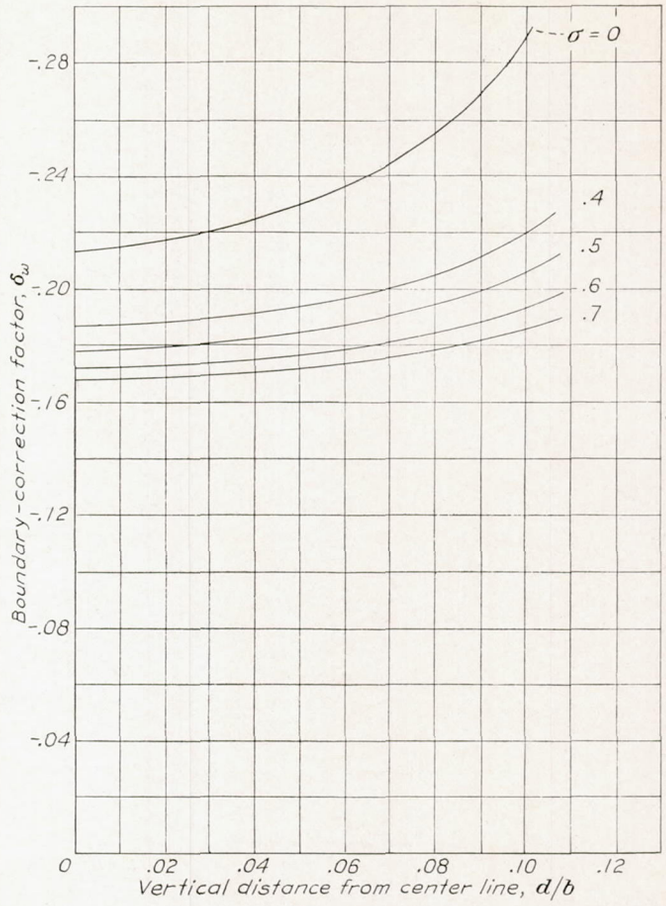

FIGURE 4.—Boundary-correction factors at the airfoil lifting line for the open 2:1 elliptical tunnel. Airfoil locations are above or below the tunnel center line.

and $\cos\alpha$ equals $\dfrac{x'-x}{\sqrt{(x'-x)^2+y'^2}}$, the downward velocity is

$$v=\frac{\Gamma}{4\pi}\frac{(x'-x)}{(x'-x)^2+y'^2}$$

in which x' and y' are constants depending on the wing position and tunnel radius, and are given by

$$x'=\frac{R^2 s}{s^2+d^2}$$

$$y'=d\left(\frac{R^2-s^2-d^2}{s^2+d^2}\right)$$

The total induced flow D over the span from both A and B is

$$D=2\int_{-s}^{s} v\,dx=\frac{\Gamma}{2\pi}\int_{-s}^{s}\frac{(x'-x)\,dx}{(x'-x)^2+y'^2}$$

$$D=\frac{\Gamma}{4\pi}\left[\log\frac{(x'+s)^2+y'^2}{(x'-s)^2+y'^2}\right]$$

Letting $\bar{v}$ be the average induced velocity over the span, $\bar{v}=\dfrac{D}{2s}$ and $\Delta\alpha_w=\dfrac{\bar{v}}{V}$. To simplify, we may write $\Gamma=\dfrac{C_L V S}{4s}$, then

$$\Delta\alpha_w=\frac{C_L S}{32\pi s^2}\left[\log\frac{(x'+s)^2+y'^2}{(x'-s)^2+y'^2}\right]=\delta_w\frac{S}{C}C_L$$

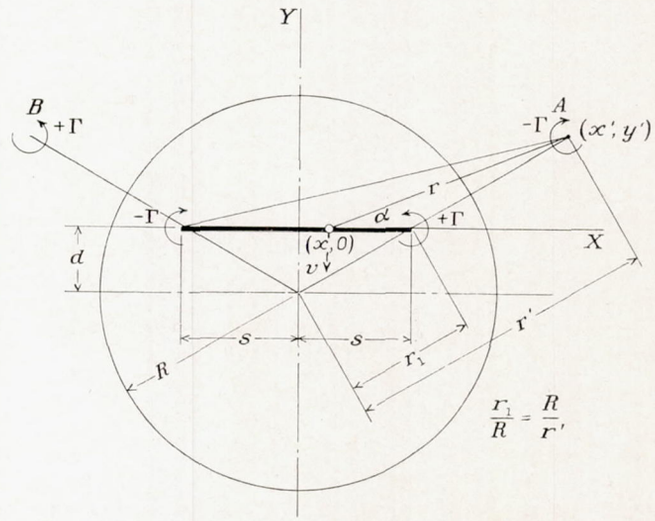

FIGURE 5.—Location of image vortices for off-center wing locations in the circular tunnel.

Since $\sigma=\frac{s}{R}$ and $C=\pi R^2$, then

$$\delta_w=\frac{1}{32\sigma^2}\left\{\log\frac{1+2\left[\sigma^2-\left(\frac{d}{R}\right)^2\right]+\left[\sigma^2+\left(\frac{d}{R}\right)^2\right]^2}{1-2\left[\sigma^2+\left(\frac{d}{R}\right)^2\right]+\left[\sigma^2+\left(\frac{d}{R}\right)^2\right]^2}\right\}$$

For an infinitely small airfoil the equation reduces to

$$\delta_w=\frac{1}{8\left[1-\left(\frac{d}{R}\right)^2\right]^2}$$

The boundary-correction factors δ_w for off-center positions in the circular tunnel are given in figure 6.

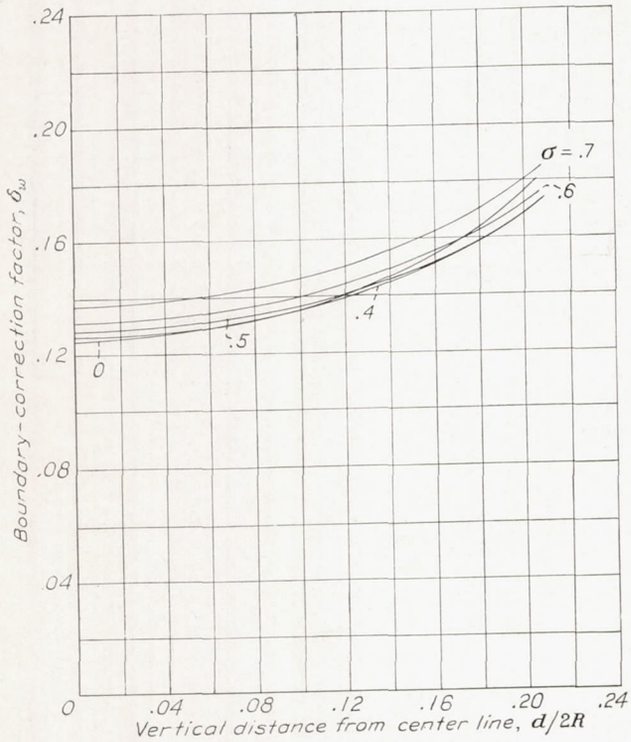

FIGURE 6.—Boundary-correction factors at the airfoil lifting line for the open and closed circular tunnels. The factor δ_w is positive for the closed tunnel and negative for the open. Airfoil locations are above or below the tunnel center line.

As a check, the values were computed by both the methods described. Numerically, they are the same for open and closed circular tunnels but are of positive sign (upwash) for the closed and negative (downwash) for the open.

Rectangular tunnel.—The images that satisfy the boundary conditions of the rectangular tunnel are arranged in a checkerboard pattern of vortices extending to infinity. The circulation strength of the images corresponds to that of the airfoil. For the closed tunnel the condition of zero velocity normal to the wall is satisfied by alternate horizontal rows of positive and negative vortices (fig. 7); in the free jet the uniform-pressure criterion is met by alternate vertical rows of positive and negative images (fig. 8). When the airfoil is not on the tunnel center line, the pattern becomes asymmetrical with regard to the origin, but the boundary conditions are fulfilled if the wing vortex is repeatedly reflected in the boundaries. Figure 9 shows the pattern for the closed rectangular tunnel with the wing above the tunnel center line. If the images are divided into two superimposed groups, one with origin at the airfoil on line A-A in figure 9 and the other with origin at the first image B-B, two symmetrical groups of images emerge with a vertical spacing of twice the tunnel height. The problem of determining the downwash at the wing is simplified and expedited since Theodorsen (reference 6) gives the equation for the group with the origin at the airfoil (line A-A) directly as

$$\delta_{w_1}=-\frac{1}{4\pi r_1\sigma^2}\left[\log\frac{\sinh\pi r_1\sigma}{\pi r_1\sigma}+\sum_1^\infty(-1)^n\log\left(1-\frac{\sinh^2\pi r_1\sigma}{\sinh^2\pi n r_1}\right)\right] \tag{3}$$

for the open tunnel, in which r_1 is the ratio of tunnel width to the doubled height, and σ is the ratio of the span of the tip vortices to the tunnel width. If we write

$$\Delta\alpha_{w_1}=\delta_{w_1}\frac{S}{C}C_L$$

the effective value of the jet area C, owing to the doubled effective tunnel height, becomes twice the true area and the values of δ_{w_1} from equation (3) must be halved for application to the true tunnel. Equation (3) as written applies to the open tunnel; the closed-tunnel values are obtained by deleting from the summation the factor $(-1)^n$, which takes into account the signs of the vertical rows of images, the minus sign in front being retained. It may be remarked that, whereas δ_{w_1} for the open tunnel is the same as δ_w for an open tunnel of doubled height with the wing on the center line, the same is not true of the closed tunnel, as may be seen from a study of the corresponding image patterns.

There remains, then, the problem of computing the flow over a span $2s$ at a distance y below the origin (origin on line B-B) contributed by an infinite pattern of vortices symmetrical about B-B and with vertical spacing of twice the tunnel height. By the method of Theodorsen (reference 6), the velocity function for an infinite vertical row of equidistant semi-infinite vortices at $x=0$ may be written as

$$v=\frac{\Gamma}{8h}\frac{\sinh\frac{\pi x}{h}}{\cosh\frac{\pi x}{h}-\cos\frac{\pi y}{h}}$$

in which v is the vertical velocity and $2h$ is the vertical spacing of the images.

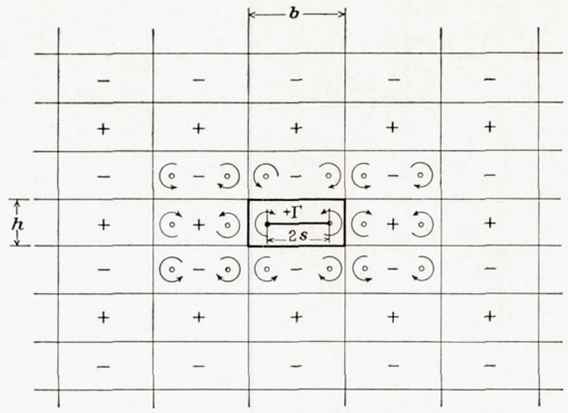

FIGURE 7.—Arrangement of the infinite image pattern to satisfy the boundary conditions of the closed rectangular tunnel.

At any value of the parameter y the stream function from this row of semi-infinite vortex filaments is evaluated by integrating with respect to x. Thus

$$\psi=\int v\,dx=\int\frac{\Gamma}{8h}\frac{\sinh\frac{\pi x}{h}}{\cosh\frac{\pi x}{h}-\cos\frac{\pi y}{h}}dx$$

integrated

$$\psi=\frac{\Gamma}{8\pi}\log\left(\cosh\frac{\pi x}{h}-\cos\frac{\pi y}{h}\right)$$

The result may now be extended to include two vertical rows of vortices of opposite sign at a distance s and

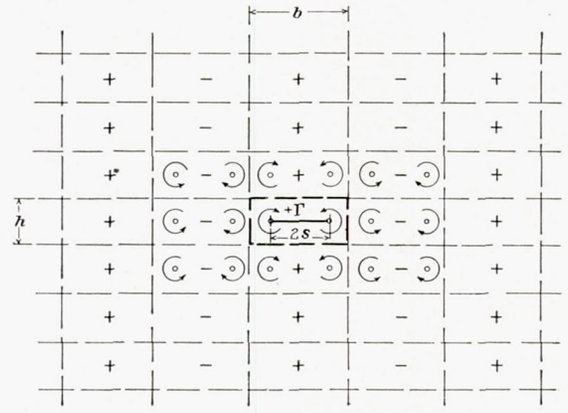

FIGURE 8.—Arrangement of the infinite image pattern to satisfy the boundary conditions of the open rectangular tunnel.

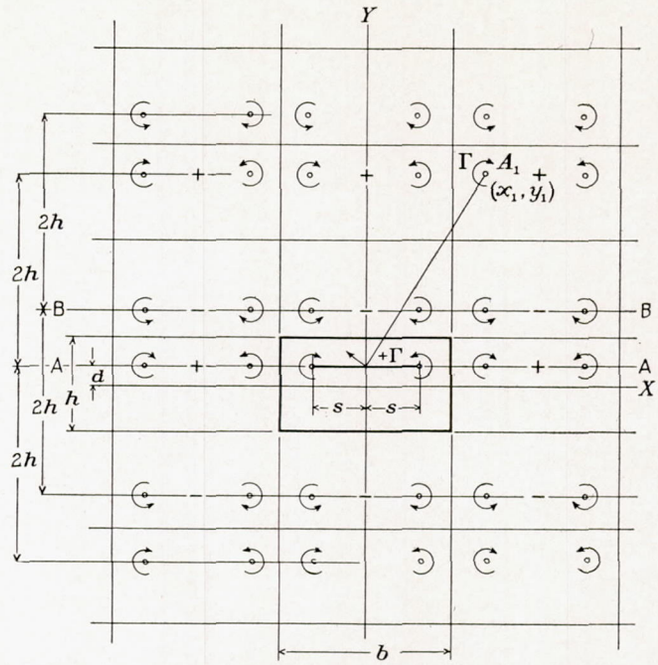

FIGURE 9.—Arrangement of the infinite image pattern to satisfy the boundary conditions for off-center locations of the wing in a closed rectangular tunnel.

$-s$ from the y axis. The stream function then becomes

$$\psi=\frac{\Gamma}{8\pi}\left\{\log\left[\cosh\frac{\pi(x-s)}{h}-\cos\frac{\pi y}{h}\right]-\log\left[\cosh\frac{\pi(x+s)}{h}-\cos\frac{\pi y}{h}\right]\right\}$$

$$\psi=-\frac{\Gamma}{8\pi}\log\frac{\cosh\frac{\pi(x+s)}{h}-\cos\frac{\pi y}{h}}{\cosh\frac{\pi(x-s)}{h}-\cos\frac{\pi y}{h}}\qquad(4)$$

The total vertical flow may be determined by adding the effect of all the double rows of vortices to infinity. The contribution to the vertical flow of any double row of vortices, say the nth, is numerically the same as the vertical flow at the location of the nth row induced by the double row at the origin. It is therefore only necessary to calculate the flow induced by this double row at the origin, between the limits

$$x=nb-s \text{ and } x=nb+s$$

For the actual vertical flow at the first exterior row of vortices with center at $x=b$, the limits $x=b-s$ and $x=b+s$ are substituted in equation (4). The vertical flow from this row is, disregarding signs,

$$D=\frac{\Gamma}{8\pi}\log\frac{\left[\cosh\frac{\pi(b+2s)}{h}-\cos\frac{\pi y}{h}\right]\left[\cosh\frac{\pi(b-2s)}{h}-\cos\frac{\pi y}{h}\right]}{\left(\cosh\frac{\pi b}{h}-\cos\frac{\pi y}{h}\right)^2}$$

For the nth double row, consequently

$$D=\frac{\Gamma}{8\pi}\log\frac{\left[\cosh\frac{\pi(nb+2s)}{h}-\cos\frac{\pi y}{h}\right]\left[\cosh\frac{\pi(nb-2s)}{h}-\cos\frac{\pi y}{h}\right]}{\left(\cosh\frac{\pi nb}{h}-\cos\frac{\pi y}{h}\right)^2}$$

The entire vertical flow for all the rows from $x=-\infty$ to $+\infty$ becomes

$$D=-\frac{\Gamma}{8\pi}\sum_{-\infty}^{\infty}\log\frac{\left[\cosh\frac{\pi(nb+2s)}{h}-\cos\frac{\pi y}{h}\right]\left[\cosh\frac{\pi(nb-2s)}{h}-\cos\frac{\pi y}{h}\right]}{\left(\cosh\frac{\pi nb}{h}-\cos\frac{\pi y}{h}\right)^2}$$

or $\frac{\Gamma}{8\pi}\psi$ in which ψ represents the negative of the infinite sum. We may write

$$2s\Gamma\rho V=\frac{1}{2}C_L\rho V^2S$$

in which V is the velocity, ρ the density of the medium, and S is the airfoil area. Simplifying,

$$\Gamma=\frac{C_LVS}{4s}$$

The angular deflection caused by the induced flow is designated

$$\Delta\alpha=\frac{\bar{v}}{V}=\frac{D}{2sV}=\frac{C_LS}{64s^2\pi}\psi=\delta\frac{S}{C}C_L$$

or with $bh=C$, the cross-sectional area of the jet; $\frac{b}{h}=r$, the ratio of the tunnel width to height; and σ equals the ratio of vortex span $2s$ to the tunnel width b; the final result for the group with origin at B–B may be written for the open tunnel

$$\delta_{w_2}=-\frac{1}{16\sigma^2\pi r}\sum_{-\infty}^{\infty}(-1)^n\log\frac{\left[\cosh\pi r(n+\sigma)+\cos 2\pi r\frac{d}{b}\right]\left[\cosh\pi r(n-\sigma)+\cos 2\pi r\frac{d}{b}\right]}{\left(\cosh\pi nr+\cos 2\pi r\frac{d}{b}\right)^2} \tag{5}$$

The summation converges rapidly and the terms for values of n greater than 2 are negligible. The same equation applies for the closed tunnel except that the factor $(-1)^n$ is omitted and the sign before the expression becomes positive.

For an infinitely small wing, equations (3) and (5) reduce to

$$\delta_1=-\frac{\pi r}{4}\left(\frac{1}{6}-\sum_{n=1}^{\infty}\frac{(-1)^n}{\sinh^2\pi nr}\right)$$

$$\delta_2=-\frac{\pi r}{16}\sum_{n=-\infty}^{\infty}(-1)^n\left[\frac{1+\cosh\pi nr\cos 2\pi r\frac{d}{b}}{\left(\cosh\pi nr+\cos 2\pi r\frac{d}{b}\right)^2}\right]$$

The total boundary-correction factor at the airfoil is

$$\delta_w=\frac{1}{2}\delta_{w_1}+\delta_{w_2} \tag{6}$$

By means of the foregoing equations the correction factors δ_w have been computed over a practical range of span ratios and wing positions for the square and 2:1 rectangular tunnels with open and closed test sections. These results are presented in figures 10 to 13, inclusive. Wing locations and effective spans are expressed as fractions of the tunnel width b.

BOUNDARY INFLUENCE AFT OF THE AIRFOIL IN RECTANGULAR TUNNELS

Thus far consideration has been given only to the conditions at a plane through the lifting line of the wing, where the transverse portion of the horseshoe vortex representing the effect of the wing does not affect the boundary condition and the problem reduces to that of finding the effect of vortices extending from zero to infinity in only one direction. If the induced vertical velocity due to the boundary interference were constant along the tunnel axis, the only effect of the interference would be to change the general direction of the air stream with respect to the airplane and balance system without in any way changing the local flow over the airplane for any given attitude with respect to the relative wind. The tunnel-wall interference, however, is not constant along the tunnel axis. The variation of boundary influence with distance downstream causes the tail of the airplane to be operating at a different angle of attack than it would in free air for the same angle of the wing to the relative wind, the discrepancy being equal to the difference in

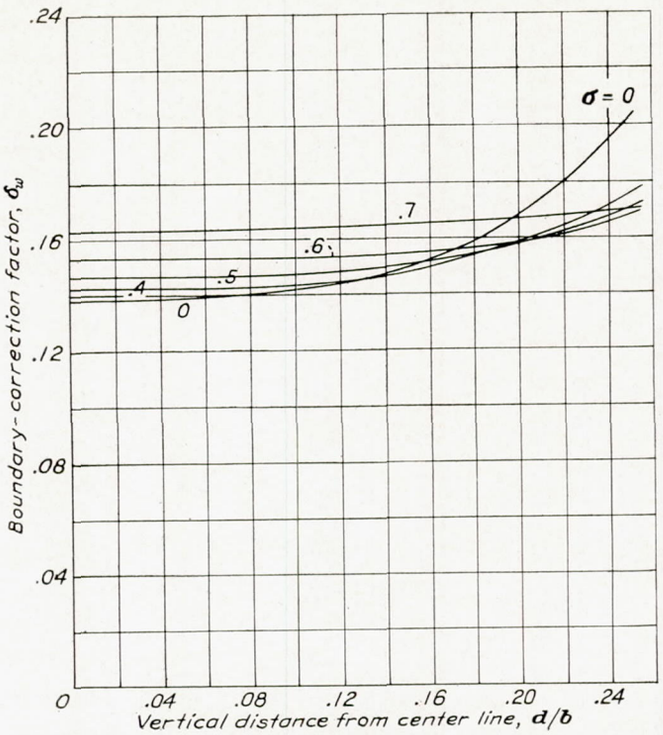

FIGURE 10.—Boundary-correction factors at the airfoil lifting line for the closed square tunnel. Airfoil locations are above or below the tunnel center line.

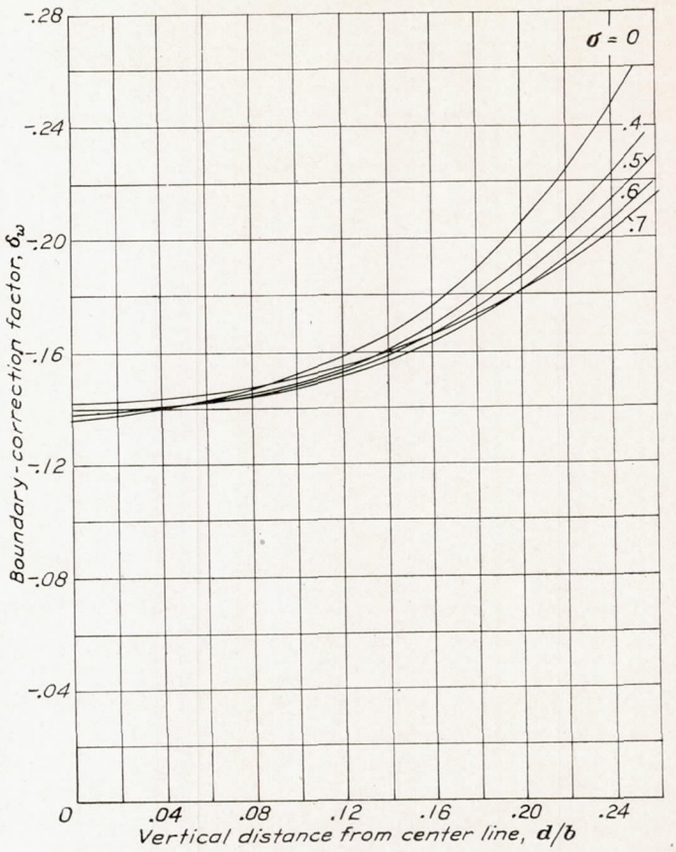

FIGURE 11.—Boundary-correction factors at the airfoil lifting line for the open square tunnel. Airfoil locations are above or below the tunnel center line.

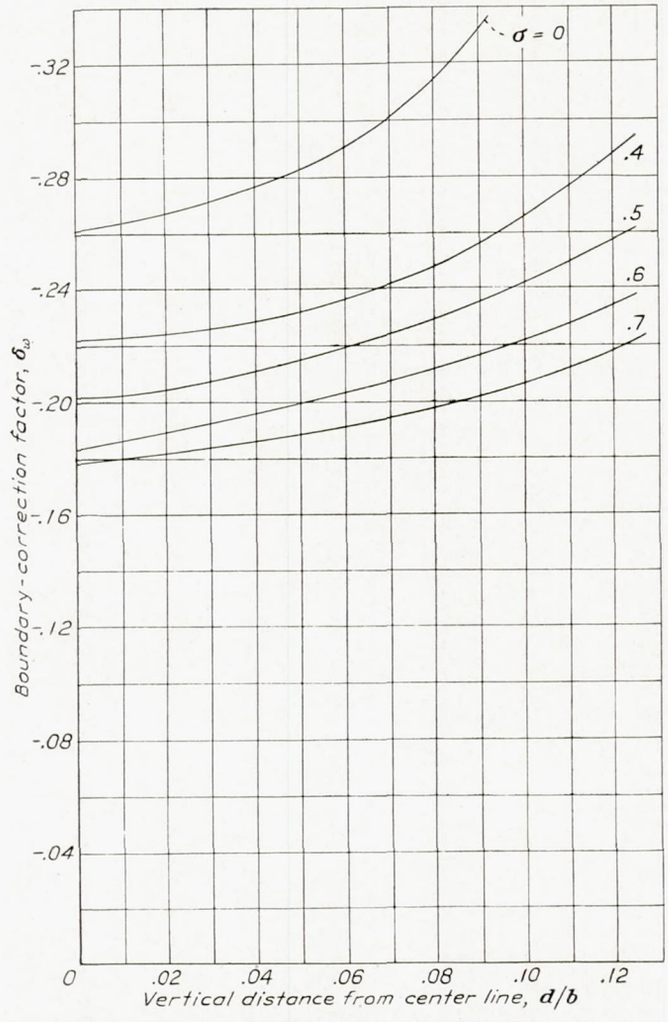

FIGURE 13.—Boundary-correction factors at the airfoil lifting line for the open 2:1 rectangular tunnel. Airfoil locations are above or below the tunnel center line.

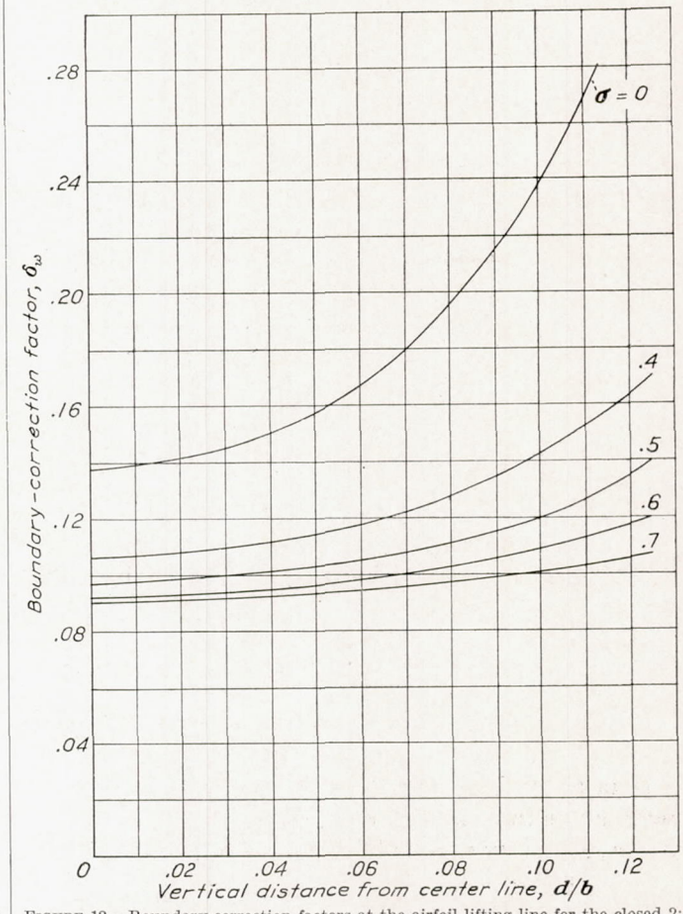

FIGURE 12.—Boundary-correction factors at the airfoil lifting line for the closed 2:1 rectangular tunnel. Airfoil locations are above or below the tunnel center line.

the induced angle of flow at the wing and tail. The tail surface also acts as an airfoil affecting the boundary conditions but the tail area is so small that this effect may be neglected.

At any cross-sectional plane behind the lifting line, the influence of the horseshoe vortex system at the tunnel boundary differs from that at the wing owing to the transverse and longitudinal segments of the wing horseshoe vortex system that extend between the wing and this plane. The longitudinal vortices downstream from the plane may still be considered to be of infinite length. A corresponding variation in the influence of the images is required in order that the boundary conditions may be satisfied.

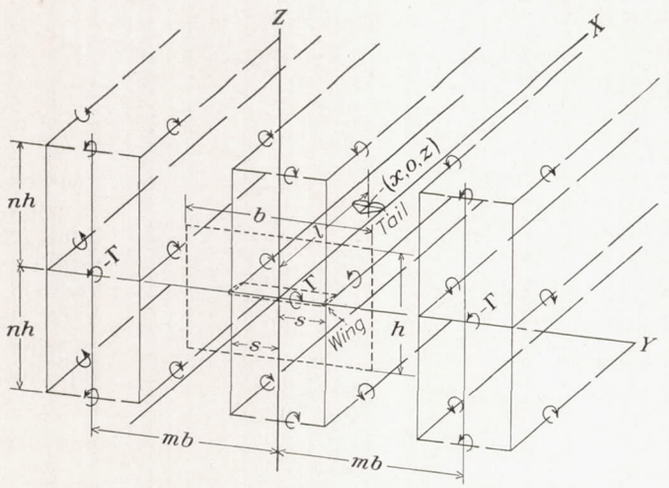

FIGURE 14.—Three-dimensional arrangement of wing and image vortices to satisfy the boundary conditions aft of the airfoil for the open rectangular tunnel.

No simple extension of the image system has been found for the circular or elliptical tunnels that satisfies the boundary conditions at all points. For the rectangular tunnel, it can easily be seen that the boundary condition is satisfied at all points by the same system of images as in the two-dimensional problem, each pair of vortices including a transverse segment to make it a complete image of the horseshoe vortex representing the wing (fig. 14). At an infinite distance behind the airfoil, the induced velocities from the transverse images become zero and the total induced velocity from the longitudinal branches, which may then be considered as extending to infinity in both fore and aft directions, reaches twice the value at the wing.

If the increment of induced angle at points behind the wing be designated $\Delta\alpha_A$, the total influence at any location from the boundaries is

$$\Delta\alpha_T=\Delta\alpha_w+\Delta\alpha_A$$

in which $\Delta\alpha_w$ is the value at the wing, from the foregoing discussion of downflow at the lifting line.

If the origin of coordinates is chosen at the center of the airfoil lifting line with the x axis coincident with the horizontal axis of the jet, the y axis along the span, and the z axis vertical, a doubly infinite series of images is located at points $y=mb$ and $z=nh$ for a rectangular tunnel of breadth b and height h (fig. 14). The variables m and n assume all positive and negative integral values except (0, 0).

Although the pattern is infinite, the images adjacent to the tunnel boundaries are the most effective and the first two rows of images exterior to the tunnel boundaries ordinarily contribute more than 90 percent of the induced flow. The validity of this statement is demonstrated by the rapidity with which the series representing the effects of consecutive rows converge and by computations showing the negligible contributions from the exterior rows.

The method followed in this paper has therefore been to determine exactly and individually the induced vertical velocity from each vortex in the first two exterior double rows of images and to sum the effects of the remaining rows to infinity by an approximate method demonstrated in reference 10.

For the additional vertical velocity w_{A_1} at a point (x, o, o) contributed by an image with circulation Γ located at (y, z), we may readily write

$$w_{A_1}=\frac{\Gamma}{4\pi}\frac{xy}{\sqrt{x^2+y^2+z^2}}\left(\frac{1}{x^2+z^2}+\frac{1}{y^2+z^2}\right) \qquad (7)$$

Since

$$\Gamma=\frac{C_L VS}{4s} \text{ and } \frac{w_{A_1}}{V}=\Delta\alpha_{A_1}$$

$$\frac{4\pi w_{A_1}}{\Gamma}=\frac{16\pi s\Delta\alpha_{A_1}}{C_L S}$$

and

$$\Delta\alpha_{A_1}=\left(\frac{4\pi w_{A_1}}{\Gamma}\right)\frac{C_L S}{16\pi s}$$

If

$$h=\lambda b \text{ and } C=\lambda b^2$$

$$\Delta\alpha_{A_1}=\frac{\left(\frac{4\pi w_{A_1}}{\Gamma}\right)\lambda b^2}{16\pi s}\frac{S}{C}C_L$$

which may be written

$$\Delta\alpha_{A_1}=\delta_{A_1}\frac{S}{C}C_L$$

therefore

$$\delta_{A_1}=\frac{\left(\frac{4\pi w_A}{\Gamma}\right)\lambda b^2}{16\pi s}$$

If the term $\left(\frac{4\pi w_{A_1}}{\Gamma}\right)$ be evaluated by equation (7) for each of the vortices in the first two exterior double rows, with positive sign for images that create upflow in the tunnel and negative for those inducing downflow, we may express the correction factor that accurately repre-

sents more than 90 percent of the interference flow as

$$\delta_{A_1}=\frac{\lambda b^2}{16\pi s}\sum_{A_1}\frac{4\pi w_{A_1}}{\Gamma} \tag{8}$$

For the remaining rows to infinity the equation for the closed tunnel may be written by the approximate method of reference 10 as

$$\Delta\alpha_{A_2}=\frac{xS}{2hC}C_L\left[\left(\frac{\lambda^2}{\pi}\right)\sum_{m=3}^{\infty}\sum_{n=1}^{\infty}(-1)^n\frac{m^2-2\lambda^2n^2}{(m^2+\lambda^2n^2)^{5/2}}+\left(\frac{\lambda^2}{\pi}\right)\sum_{m=1}^{2}\sum_{n=3}^{\infty}(-1)^n\frac{m^2-2\lambda^2n^2}{(m^2+\lambda^2n^2)^{5/2}}+\frac{\lambda^2}{2\pi}\sum_{3}^{\infty}\frac{1}{m^3}+\frac{1}{\lambda\pi}\sum_{3}^{\infty}\frac{(-1)^{n+1}}{n^3}\right] \tag{9}$$

and for the open tunnel

$$\Delta\alpha_{A_2}=\frac{xS}{2hC}C_L\left[\left(\frac{\lambda^2}{\pi}\right)\sum_{m=3}^{\infty}\sum_{n=1}^{\infty}(-1)^m\frac{m^2-2\lambda^2n^2}{(m^2+\lambda^2n^2)^{5/2}}+\left(\frac{\lambda^2}{\pi}\right)\sum_{m=1}^{2}\sum_{n=3}^{\infty}(-1)^m\frac{m^2-2\lambda^2n^2}{(m^2+\lambda^2n^2)^{5/2}}+\frac{\lambda^2}{2\pi}\sum_{3}^{\infty}\frac{(-1)^m}{m^3}-\frac{1}{\lambda\pi}\sum_{3}^{\infty}\frac{1}{n^3}\right] \tag{10}$$

The assumptions are made that the wing may be represented by a doublet at the center of the jet and that the distances to the exterior vortices are large compared with the span $2s$ and the distance along the axis x. Positive values of $\Delta\alpha_{A_2}$ indicate upflow in the tunnel.

If the terms in the brackets of equations (9) and (10) are denoted by ψ, then

$$\Delta\alpha_{A_2}=\frac{xS}{2hC}C_L\psi$$

or

$$\Delta\alpha_{A_2}=\delta_{A_2}\frac{S}{C}C_L$$

and

$$\delta_{A_2}=\frac{x\psi}{2b\lambda}$$

The total increment of induced angle behind the airfoil is

$$\Delta\alpha_A=\Delta\alpha_{A_1}+\Delta\alpha_{A_2}$$

therefore

$$\delta_A=\delta_{A_1}+\delta_{A_2}$$

The values of δ_A in terms of the wing correction δ_w are presented in figures 15 to 26 for the open and closed square tunnels and for the 2:1 rectangular tunnels. They cover a practical range of wing and tail positions in the test section. The wing positions and distances to the rear are given as fractions of the tunnel breadth b. The tail heights for a particular wing height correspond to the positions that the tail occupies over a range of angles of attack of the airplane thrust axis.

Although no theoretical solution has been made, it is believed that the values of δ_A/δ_w for the square and the 2:1 rectangular tunnels apply to the circular and 2:1 elliptical tunnels, respectively, with an accuracy sufficient for practical use.

A special case of some interest is that of a wing at the center and extending through the walls of a closed rectangular tunnel. For this case there are no trailing vortices and therefore there is no induced vertical velocity at the plane of the wing due to boundary interference. There is, however, an interference at downstream points from the images of the transverse vortex and, since this interference varies with distance along the tunnel, there is an effective curvature of the air stream.

Since a wing spanning a closed rectangular tunnel may be considered the same as an infinitely long wing between an upper and lower boundary, the image system consists simply of a single vertical row of infinite transverse vortices of alternating signs with a vertical spacing equal to the height of the tunnel. The vertical velocity due to the nth image vortex above the wing at any point x downstream from the airfoil lifting line and z above the center of the tunnel is

$$w=-\frac{\Gamma}{2\pi}\frac{(-1)^n x}{(nh-z)^2+x^2}$$

The total induced velocity is that from all the vortices from $n=-\infty$ to $n=+\infty$ except the one at $n=0$, which is that of the wing itself. Or,

$$w=-\frac{\Gamma}{2\pi}\left[\sum_{-\infty}^{\infty}\frac{(-1)^n x}{(nh-z)^2+x^2}-\frac{x}{z^2+x^2}\right] \tag{11}$$

If only points along the center of the tunnel are of interest, $z=0$ and (11) reduces to

$$w=-\frac{\Gamma}{2\pi}\left[\sum_{-\infty}^{\infty}(-1)^n\frac{x}{x^2+n^2h^2}-\frac{1}{x}\right]$$

which can be expressed very simply as

$$w=-\frac{\Gamma}{2\pi}\left(\frac{\frac{\pi}{h}}{\sinh\frac{\pi x}{h}}-\frac{1}{x}\right)$$

(See reference 5.)

Putting $\Gamma=\frac{C_L VS}{4s}$ and $\Delta\alpha=\frac{w}{V}$

$$\Delta\alpha_A=-\frac{C_L S}{8sh}\left(\frac{1}{\sinh\pi\frac{x}{h}}-\frac{1}{\pi\frac{x}{h}}\right)$$

$$\delta_A=-\frac{1}{4}\left(\frac{1}{\sinh\pi\frac{x}{h}}-\frac{1}{\pi\frac{x}{h}}\right)$$

If c is the chord of the airfoil

$$\Delta\alpha_A=\delta_A\frac{S}{C}C_L=\delta_A\frac{c}{h}C_L$$

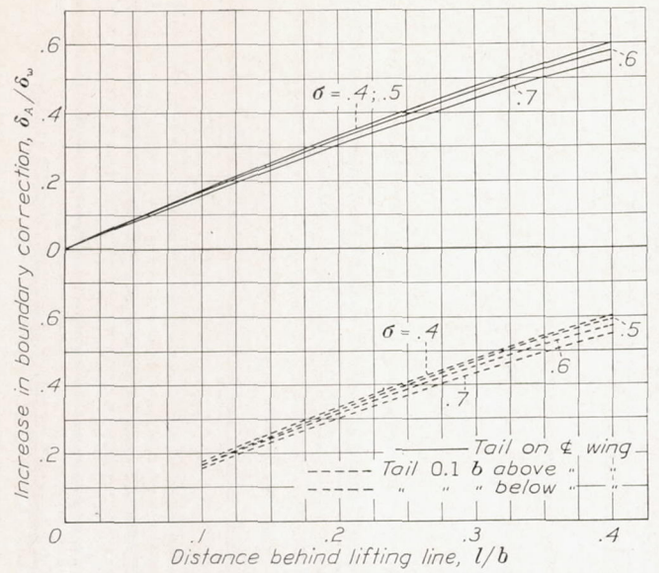

FIGURE 15.—Boundary-correction factors aft of the airfoil lifting line for the closed square tunnel with wing on tunnel center line. Value of δ_w from figure 10.

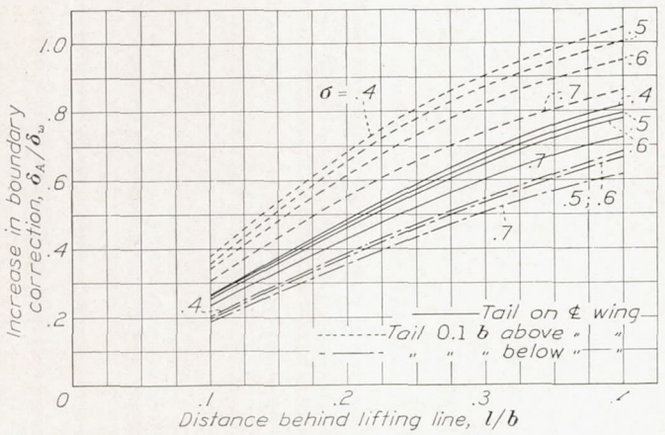

FIGURE 17.—Boundary-correction factors aft of the airfoil lifting line for the closed square tunnel with wing 0.2 b above tunnel center line. Value of δ_w from figure 10.

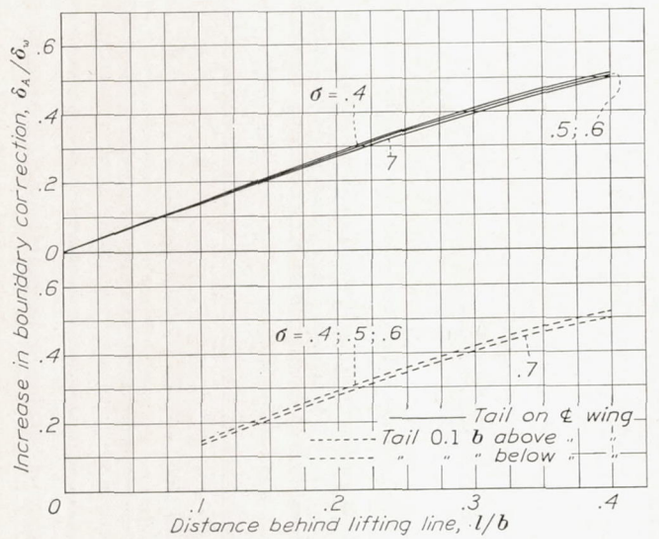

FIGURE 18.—Boundary-correction factors aft of the airfoil lifting line for the open square tunnel with wing on tunnel center line. Value of δ_w from figure 11.

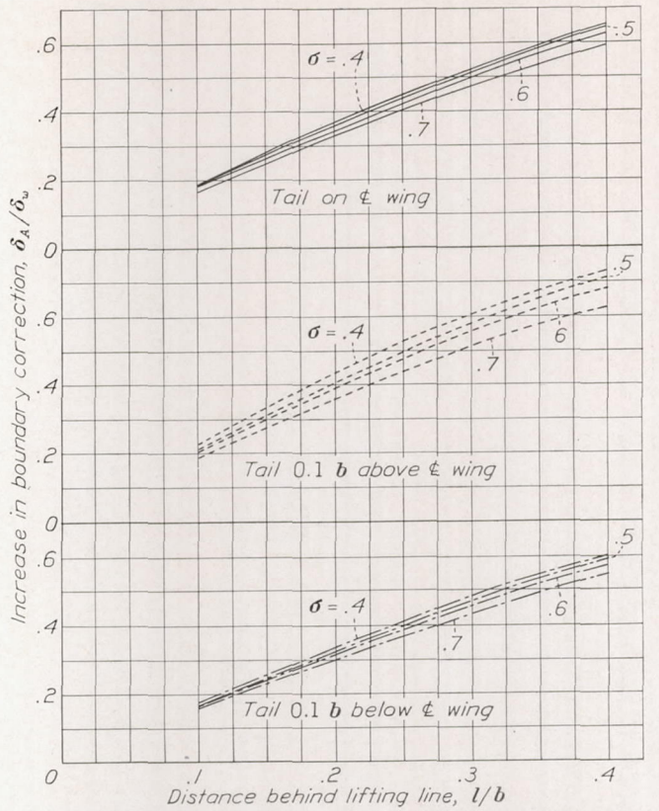

FIGURE 16.—Boundary-correction factors aft of the airfoil lifting line for the closed square tunnel with wing 0.1 b above tunnel center line. Value of δ_w from figure 10.

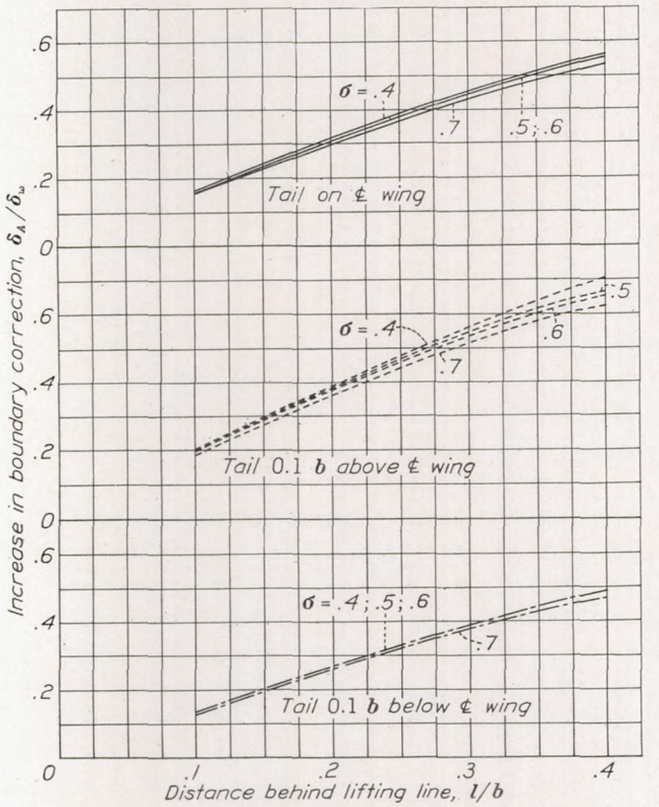

FIGURE 19.—Boundary-correction factors aft of the airfoil lifting line for the open square tunnel with wing 0.1 b above tunnel center line. Value of δ_w from figure 11.

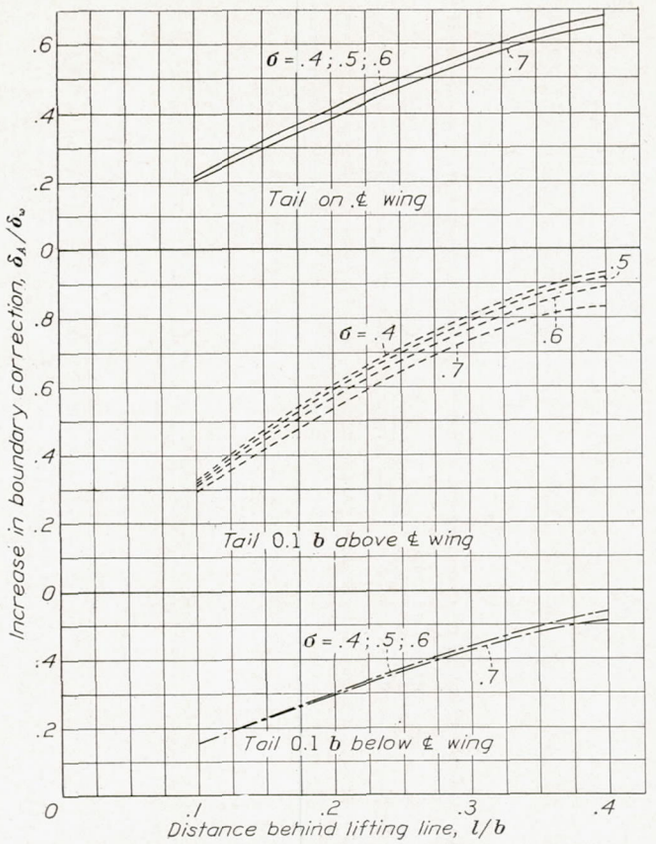

FIGURE 20.—Boundary-correction factors aft of the airfoil lifting line for the open square tunnel with wing 0.2 b above tunnel center line. Value of δ_w from figure 11.

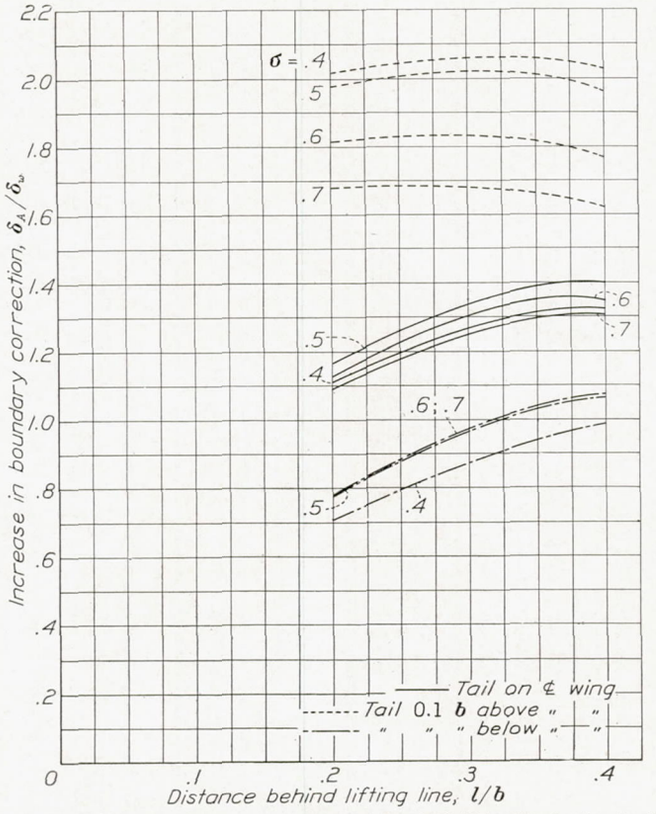

FIGURE 23.—Boundary-correction factors aft of the airfoil lifting line for the closed 2:1 rectangular tunnel with wing 0.1 b above tunnel center line. Value of δ_w from figure 12.

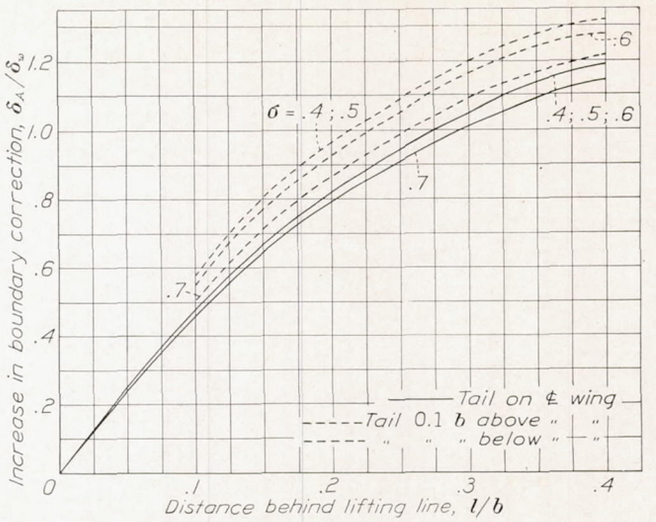

FIGURE 21.—Boundary-correction factors aft of the airfoil lifting line for the closed 2:1 rectangular tunnel with wing on tunnel center line. Value of δ_w from figure 12.

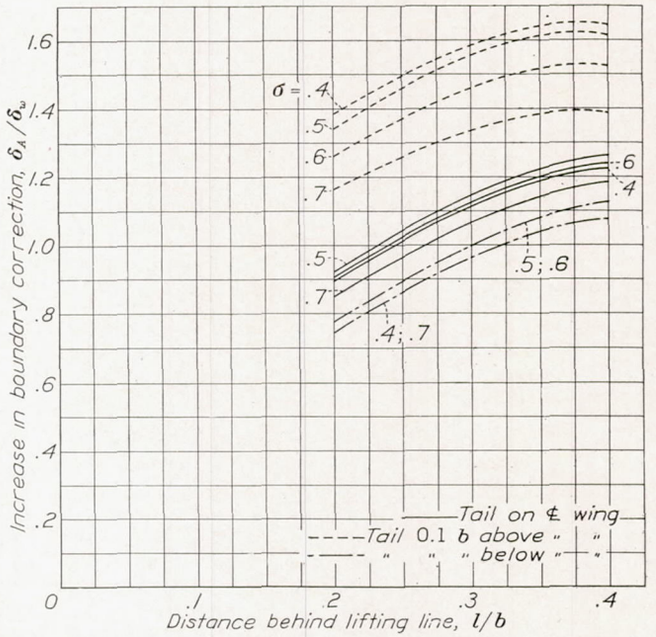

FIGURE 22.—Boundary-correction factors aft of the airfoil lifting line for the closed 2:1 rectangular tunnel with wing 0.05 b above tunnel center line. Value of δ_w from figure 12.

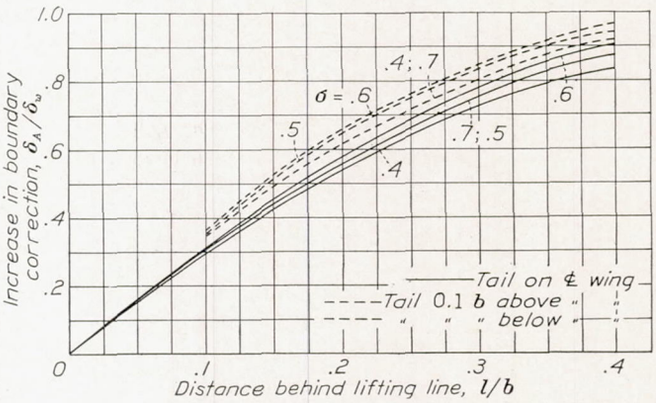

FIGURE 24.—Boundary-correction factors aft of the airfoil lifting line for the open 2:1 rectangular tunnel with wing on tunnel center line. Value of δ_w from figure 13.

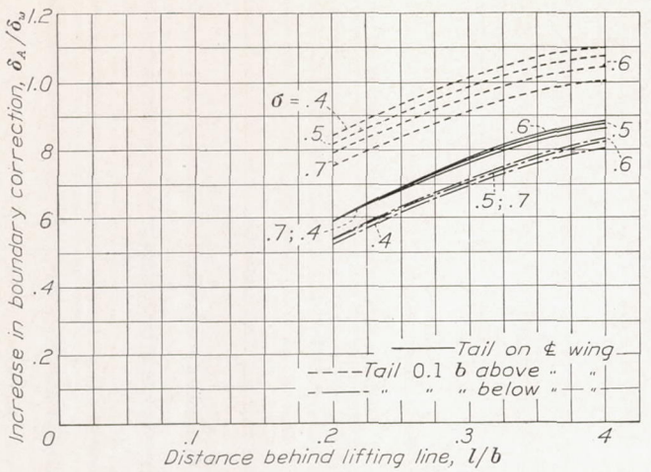

FIGURE 25.—Boundary-correction factors aft of the airfoil lifting line for the open 2:1 rectangular tunnel with wing 0.05 b above tunnel center line. Value of δ_w from figure 13.

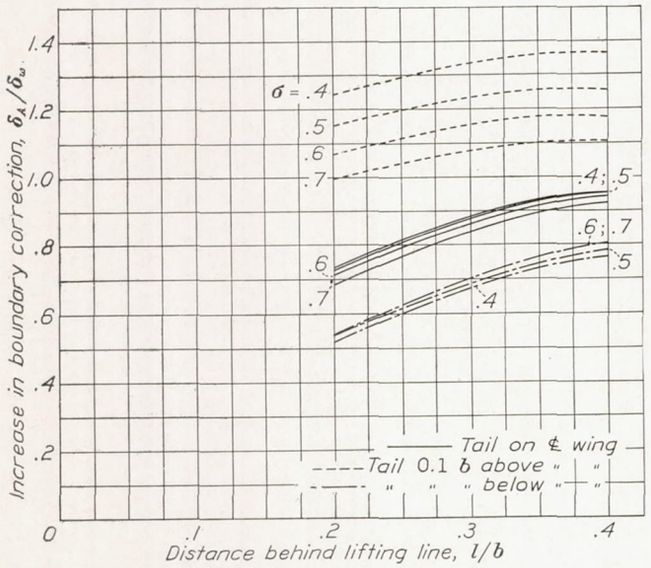

FIGURE 26.—Boundary-correction factors aft of the airfoil lifting line for the open 2:1 rectangular tunnel with wing 0.1 b above tunnel center line. Value of δ_w from figure 13.

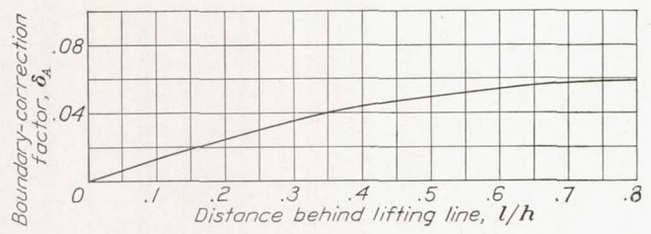

FIGURE 27.—Boundary-correction factors aft of the infinite span airfoils in closed rectangular tunnels. δ_w is zero.

The values of δ_A are plotted against distance downstream in figure 27. They are small as compared with the corrections obtained for finite wings. It may be noted that these corrections are independent of the height-breadth ratio of the tunnel and may be used for closed rectangular tunnels of any dimensions.

It is expected that these results for the boundary influence behind the wing will check experimental results for closed rectangular tunnels. In the case of open tunnels, however, the problem is not so definite because other factors, such as the proximity to and shape of the exit cone, may seriously alter the flow behind the wing. Thus it is desirable to verify the validity of the results for any given open tunnel.

LANGLEY MEMORIAL AERONAUTICAL LABORATORY,
NATIONAL ADVISORY COMMITTEE FOR AERONAUTICS,
LANGLEY FIELD, VA., *June 28, 1935.*

REFERENCES

1. Prandtl, L.: Tragflügeltheorie. II C, Göttingen Nachrichten, 1919.
2. Glauert, H.: The Elements of Aerofoil and Airscrew Theory. Chaps. XII and XIV, Cambridge University Press, 1926.
3. Glauert, H.: The Interference on the Characteristics of an Aerofoil in a Wind Tunnel of Rectangular Section. R. & M. No. 1459, British A. R. C., 1932.
4. Terazawa, Kwan-ichi: On the Interference of Wind Tunnel Walls of Rectangular Cross-Section on the Aerodynamical Characteristics of a Wing. Report No. 44, Aero. Res. Inst., Tokyo Imperial University, 1928.
5. Theodorsen, Theodore: The Theory of Wind-Tunnel Wall Interference. T. R. No. 410, N. A. C. A., 1931.
6. Theodorsen, Theodore: Interference on an Airfoil of Finite Span in an Open Rectangular Wind Tunnel. T. R. No. 461, N. A. C. A., 1933.
7. Rosenhead, L.: The Effect of Wind Tunnel Interference on the Characteristics of an Aerofoil. Roy. Soc. Proc., Math. and Phys., 129A, (London), 1930, pp. 115–135.
8. Tani, Itiro, and Sanuki, Matao: The Wall Interference of a Wind Tunnel of Elliptic Cross Section. Proceedings of the Physics-Math. Soc. of Japan, 3d Series, vol. 14, no. 10, 1932.
9. Theodorsen, Theodore, and Silverstein, Abe: Experimental Verification of the Theory of Wind-Tunnel Boundary Interference. T. R. No. 478, N. A. C. A., 1934.
10. Glauert, H., and Hartshorn, A. S.: The Interference of Wind Channel Walls on the Downwash Angle and the Tail setting to Trim. R. & M. No. 947, British A. R. C., 1924.

U. S. GOVERNMENT PRINTING OFFICE: 1936

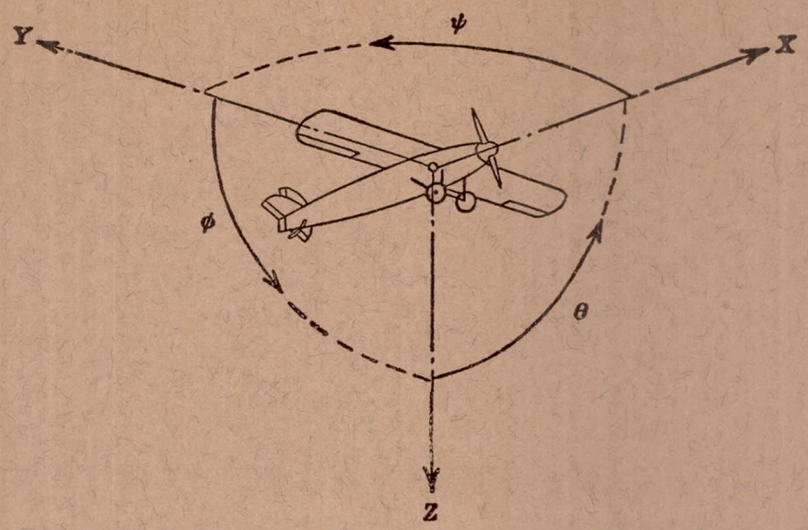

Positive directions of axes and angles (forces and moments) are shown by arrows

Axis		Force (parallel to axis) symbol	Moment about axis			Angle		Velocities	
Designation	Symbol		Designation	Symbol	Positive direction	Designation	Symbol	Linear (component along axis)	Angular
Longitudinal	X	X	Rolling	L	$Y \longrightarrow Z$	Roll	ϕ	u	p
Lateral	Y	Y	Pitching	M	$Z \longrightarrow X$	Pitch	θ	v	q
Normal	Z	Z	Yawing	N	$X \longrightarrow Y$	Yaw	ψ	w	r

Absolute coefficients of moment

$C_l = \frac{L}{qbS}$ (rolling) $\quad C_m = \frac{M}{qcS}$ (pitching) $\quad C_n = \frac{N}{qbS}$ (yawing)

Angle of set of control surface (relative to neutral position), δ. (Indicate surface by proper subscript.)

4. PROPELLER SYMBOLS

D, Diameter

p, Geometric pitch

p/D, Pitch ratio

V', Inflow velocity

V_s, Slipstream velocity

T, Thrust, absolute coefficient $C_T = \frac{T}{\rho n^2 D^4}$

Q, Torque, absolute coefficient $C_Q = \frac{Q}{\rho n^2 D^5}$

P, Power, absolute coefficient $C_P = \frac{P}{\rho n^3 D^5}$

C_s, Speed-power coefficient $= \sqrt[5]{\frac{\rho V^5}{P n^2}}$

η, Efficiency

n, Revolutions per second, r.p.s.

Φ, Effective helix angle $= \tan^{-1}\left(\frac{V}{2\pi r n}\right)$

5. NUMERICAL RELATIONS

1 hp. = 76.04 kg-m/s = 550 ft-lb./sec.

1 metric horsepower = 1.0132 hp.

1 m.p.h. = 0.4470 m.p.s.

1 m.p.s. = 2.2369 m.p.h.

1 lb. = 0.4536 kg.

1 kg = 2.2046 lb.

1 mi. = 1,609.35 m = 5,280 ft.

1 m = 3.2808 ft.